Am J Transl Res 2021;13(4):2365-2378
www.ajtr.org /ISSN:1943-8141/AJTR0109155

Original Article

Myocardial infarction cardiomyocytes-derived exosomal miR-328-3p promote apoptosis via Caspase signaling

Jiechun Huang, Fangrui Wang, Xiaotian Sun, Xianglin Chu, Rongrong Jiang, Yiqing Wang, Liewen Pang

Department of Cardiothoracic Surgery, Huashan Hospital of Fudan University, 12th Wulumuqi Road, Shanghai 200040, PR China

Received February 13, 2020; Accepted July 21, 2020; Epub April 15, 2021; Published April 30, 2021

Abstract: Exosomal miRNAs are used as novel non-invasive biomarkers for detection strategies of human disease. Here, we aimed to investigate the potential clinical value of exosomal miRNAs for myocardial infarction (MI) diagnosis and treatment. Differentially expressed miRNAs were obtained from normal cardiomyocytes, MI cardiomyocytes and adjacent normal cardiomyocytes using miRNA microarray analysis. Exosomes were isolated by centrifugation and identified by transmission electron microscopy (TEM) and western blot. The expression of miR-328-3p in exosomes was then verified by qRT-PCR. Cell apoptosis was measured using flow cytometry and TUNEL analysis. The MI severity was confirmed by masson's trichrome staining and echocardiography. MiR-328-3p was significantly increased in the MI cardiomyocytes and adjacent normal cardiomyocytes. We further confirmed miR-328-3p increasing in the exosomes from MI cardiomyocytes, which can be taken into normal cardiomyocytes. Furthermore, exogenous exosomal miR-328-3p increased apoptosis of cardiomyocytes and promoted MI. Genes regulated by miR-328-3p are mainly enriched in Caspase signaling, which is an important apoptosis regulating signaling pathway. Additionally, Caspase-3 inhibitor, Z-DEVD-FMK, reversed apoptosis and MI promoting function of miR-328-3p. Exosomal miR-328-3p is a potential novel diagnostic biomarker and therapeutic target for MI, and Z-DEVD-FMK could reverse the apoptosis progression induced by miR-328-3p.

Keywords: Myocardial infarction, exosomes, miR-328-3p, apoptosis, Caspase signaling

Introduction

Although the mortality rate of myocardial infarction (MI) has much improved since rapid revascularization of occluded coronary arteries became common practice, MI remains to be one of the leading causes of death and chronic heart failure [1]. Small molecule therapy has been recognized as a promising treatment option to restore damaged myocardium after MI [2]. Although there are treatments to mitigate the initial cardiac damage during an acute MI, there is a need for novel treatments to minimize subsequent cardiac remodeling that can adversely affect heart function. In this context, identifying new targets to improve tissue repair, including preservation of the cardiac microvasculature, clearance of apoptotic cells, and tissue regeneration, are of great interest [3, 4]. So far, various types of small molecule including exosomes and microRNAs (miRNAs) have been reported to reduce infarct size and improve myocardial function after MI; however, mechanisms underlying the effects of stem cell therapies remain unclear [5, 6].

Exosomes are small vesicles ranging from 30 to 100 nm in size that contain proteins, lipids, as well as various types of nucleic acids, including DNA, RNA, and miRNAs [7]. Reports have suggested that the myocardial tissue secretes exosomes, and which could be an important mechanism involved in heterocellular communication in the adult heart, especially exosomes emerging in the border zone of MI [8]. In addition, it needs to be mentioned that the type and quantity of exosomes derived from the border zone and normal myocardium were different. Kanada reported that exosomes from the same source did not deliver functional nucleic acids, suggesting the selectivity and importance of exosomal miRNA transfer [9]. In a human study, miR-1 and miR-133a are increased in serum of patients with acute coronary syndrome. Furthermore, using a mouse MI model, the authors have shown that miR-133a is released in exo-

somes from cardiamyocytes under ischemia [10]. MiR-214 has been shown to be upregulated in the heart after ischemia; it has also been shown to be secreted in exosomes from human endothelial cells [11, 12]. All the above results suggest that exosomes transport miRNA information, and different cell-derived exosomes induced selective miRNA profile expression, which may protect cell from death in the ischemia.

miRNAs are small non-coding RNAs that bind to complementary sequences on mRNAs and regulate many biological processes [13]. Many miRNAs are known to be involved in the pathophysiology of various cardiac diseases and the repair and regeneration of cardiac tissues [14]. In recent studies, miRNAs, including miRNA-15b, miRNA-34a, miRNA-92a, and miRNA-320 have been reported to be involved in the regulation of cardiomyocyte apoptosis after MI [15]. Given that paracrine factors exert anti-apoptotic effects, there may be a link between the actions of paracrine factors from transplanted stem cells and the roles of miRNAs in stem cell therapies for MI. In addition, even though a few potential mechanisms have been proposed for beneficial effects of stem cell therapies, there have been no reports related to the role of miRNAs in paracrine effect of transplanted MSC. miR-34a has been reported to activate Caspase, which initiated apoptosis. Caspases, the interleukin-1β-converting enzyme family proteases, are highly homologous to Caenorhabditis elegans cell death gene CED-3 (IRE1α cleaves select microRNAs during ER stress to derepress translation of proapoptotic Caspase-2) [16].

In the present study, our data revealed miR-328-3p was observably increased in the MI cardiomyocytes tissues and exosomes. A range of molecular biological methods were performed to detect the effect of miR-328-3p in the development and occurrence of MI, and to clarify the underlying molecular mechanisms. Our study showed that miR-328-3p might act as an apoptosis promoter in MI and provided a theoretical basis for optimizing treatment strategies.

Materials and methods

Ethical approval and mouse model of MI

All experimental procedures were performed in accordance with the ARRIVE guidelines for research [17], and the Fudan University Institutional Animal Care and Use Committee approved all protocols (2018-0054A). The recipient male BALB/C nude mice (weight 20 g to 22 g, Slaccas Animal Laboratory, Shanghai, China) were intraperitoneally anesthetized with 45 mg/kg of pentobarbital, intubated, and then ventilated at 110 breaths per min. In the sham group, mice were subjected to sham surgery followed by medium injection. In the surgery group, the left anterior descending (LAD) coronary artery was proximally ligated with an 8-0 silk suture via a left thoracotomy incision. The animals were maintained in the Fudan University Animal Experiment Center and were kept in a specific pathogen-free facility at a controlled temperature (23 ± 2°C) and humidity (55 ± 5%) with a 12 h artificial light-dark cycle.

Masson's trichrome staining and TdT-UTP nick end labeling (TUNEL) assays

For histopathology, fixed heart tissues were embedded in paraffin, and cut into 4 μm sections. Collagen in myocardium sections was stained using the Masson's trichrome method. The infarct area was measured as the percent ratio (%) of the injured area, divided by the whole myocardium area in each rat. TUNEL were performed according to the manufacturer's instructions for the one-step TUNEL kit (C1091, Beyotime, Shanghai, China). H9C2 cells were fixed onto poly-(L-lysine)-coated slides with 4% paraformaldehyde. After being rinsed by PBS, cells were permeabilized with 0.1% Triton X-100. After three times of washes by PBS, cells were incubated in 50 ml of TUNEL reaction mixture for 1 hour at 37°C in darkness. Then cells were incubated with 50 ml of DAPI for 2 min at room temperature. Fluorescence microscopy (488 nm excitation; 530 nm emissions) captured the images; green fluorescence represented TUNEL positive, apoptotic cells.

Exosome isolation and quantification

Exosomes were isolated from plasma of MI cardiomyocytes, adjacent normal cardiomyocytes and normal cardiomyocytes. After centrifuged at 3000 g for 15 min at 4°C, the supernatant was collected. A total of 250 uL of plasma was mixed with ExoQuick exosome precipitation solution (EXOQ5A-1, System Biosciences, USA) and exosome isolation was performed according to the manufacturer's instructions.

Exosomal protein was measured by the BCA™ Protein Assay Kit (23225, Pierce, USA). CD34 (1/10000, ab81289, Abcam, Uk), CD81 (1/1000, ab109201, Abcam), CD44 (1/2000, ab157107, Abcam), CD200 (1/100, ab203887, Abcam) and CD105 (1/1000, ab169545, Abcam) were used as exosomal markers for exosomes. The exosomes were used for following experiments immediately or stored at -80°C.

Transmission electron microscopy (TEM)

The exosomes were observed by TEM. Exosomes were isolated and fixed in 1% glutaraldehyde for 10 min, washed with deionized water. Approximately 10 μL of exosome suspension was placed on formvar carboncoated 300-mesh copper electron microscopy grids (CB8-2090836, SIGMA, Switzerland), and incubated for 5 min at room temperature. Then exosomes were negatively stained with 2% uranyl oxalate for 1 min at room temperature. The grids were washed with three times of PBS and air dried for 5 min. Images were obtained by TEM (JEM-2100, Jeol, Japan).

Western blot

Treated cells were collected, and lysates were prepared in lysis buffer (50 mM EDTA, 50 mM NaCl, 1% Triton X-100) containing a protease inhibitor cocktail (P1030, Beyotime, China). The protein determination method is BCA. An equal amount of total cell lysate (30 μg) was separated on 12% SDS-PAGE gels and transferred to PVDF membranes. Following antigen blocking with QuickBlock™ Blocking Buffer for western blot analysis (P0252; Beyotime Institute of Biotechnology), the membranes were incubated with primary antibodies against cleaved-Caspase 3 (1 μg/ml; ab2302, Abcam), cleaved-Caspase 3 (1/10000; ab32499, Abcam) and β-actin (1/200, ab115777, Abcam) overnight. Then, the membranes, which were rinsed with TBST, were incubated with goat anti-rabbit secondary antibody (1:1,000; A0208; Beyotime) and visualized with chemiluminescence (New England Nuclear, Boston, MA, USA) by Image Lab software (Bio-Rad Laboratories, Hercules, CA, USA). The experiments were performed in triplicate.

miRNA microarray of exosomes

Exosomes from mice MI cardiomyocytes, adjacent normal cardiomyocytes and normal cardiomyocytes were collected for microarray analysis. Agilent mouse miRNA microarray (v19.0; Agilent Technologies Inc., Santa Clara, CA, USA) was used in the analysis. miRNAs were labeled and hybridized with miRNA Complete Labeling and Hybridization kit (Agilent Technologies) according to the manufacturer's protocol. The original data files were processed by Feature Extraction software. Signals were normalized using Gene Spring GX software 11.0 (Agilent Technologies). ANOVA was used to compare the different miRNA expressions.

Exosome treatment

Exosomes were isolated from 5×10^6 MI cardiomyocytes, Cells were planted into 6-well plates one day before treatment. When the cells grew at about 70% of confluent, 200 μg of exosomes were directly added into cells. PBS was added as control. Forty-eight hours after treatment, cells were collected for the following experiments.

Quantitative real-time PCR

Total RNA was isolated from cells or exosomes using Trizol reagent (15596018, Invitrogen, USA). cDNA was synthesized from total RNA using the RevertAid First Strand cDNA Synthesis Kit (K1622, Thermo Scientific, USA) and miDETECT A TrackTM miRNA qRT-PCR starter Kit (AM1558, Invitrogen). U6 snRNA was used as an endogenous control to normalize miRNA expression in cells, and cel-miR-39 was used to normalize miRNA expression in exosomes between the samples. The primers of U6 (miRAN0002-1-200) and cel-miR-39 (MQPS000-0072-1-200) were purchased from RiboBio, China. Relative miRNA expression levels were calculated by the $2^{-\Delta\Delta Ct}$ method. All samples were tested thrice.

Echocardiography

5 weeks after MI operation, Echocardiography was performed with a 14-Hz ultrasound probe (Hewlett Packard Sonos 5500, CA, USA). Data of left ventricular end-diastolic dimension (LVEDD), heart rate and left ventricular end-systolic diameter (LVESD) were collected. In the parasternal short-axis view, the heart was firstly imaged in two-dimensional (2D) mode. From this view, an M-mode cursor was positioned perpendicular to the interventricular septum and posterior wall of the left ventricle (LV) in the

direction of the chordae tendineae. From this position, M-mode images were obtained to measure chamber dimensions and wall thickness according to the leading-edge convention adapted by the American Society of Echocardiography.

Annexin V staining

Apoptotic cells were quantified using the Fluorescin isothiocyanate (FITC) annexin V apoptosis detection kit 1 (BD Biosciences Pharmingen, San Diego, CA, USA), according to the manufacturer's instructions. The trypsinized cells were stained with FITC annexin V and propidium iodide (PI) and then analyzed by flow cytometry using a BD FACS Canto (BD Biosciences, San Jose, CA, USA). The total area of annexin V positive cardiomyocytes was determined by computerized morphometry (BD FACS Diva software).

Statistical analysis

All statistical analyses were performed using the SPSS 21.0 software, and the graphs were generated using GraphPad Prism 6.0 (GraphPad Software, San Diego, CA, USA). All data are presented as the mean ± SD and were analyzed by the means of two-tailed independent sample one-way ANOVA, chi-square test and Student's t-test. The *p*-values were two-sided, and the value of 0.05 was defined as statistically significant.

Results

Identifying exosomal miRNAs secreted from cardiomyocytes during MI

We first determined the effects of LAD coronary artery ligation in mice model establishment. The mice that received LAD coronary artery ligation surgery developed larger necrosis area compared to control group alone (**Figure 1A**). The result indicates that MI mice model were established successfully. We next examined the miRNA profile of normal cardiomyocytes and MI cardiomyocytes. miRNA expression profiling revealed that 54 miRNAs were significantly increased and 98 miRNAs were significantly decreased in the MI cardiomyocytes compared to normal cardiomyocytes. Some exosomal miRNAs including miR-328-3p, miR-326-3p, miR-210-3p, miR-574-3p, miR-5100, miR-193a-3p, miR-146a-5p, miR-573-5p, miR-632-3p, miR-8101-3p and miR-1904-3p were increased, while others such as miR-110-5p, miR-653-3p, miR-27a-3p, miR-25-3p, miR-6418-5p, miR-6003, miR-4119, miR-3102-5p and miR-5113 were decreased by more than 2-fold in MI tissues compared to normal cardiomyocytes (**Figure 1B**). We also examined the miRNA profile of normal cardiomyocytes and adjacent cardiomyocytes to MI tissues. miRNA expression profiling revealed that 63 miRNAs were significantly increased and 76 miRNAs were significantly decreased in the adjacent cardiomyocytes compared to normal cardiomyocytes. Some exosomal miRNAs including miR-328-3p, miR-7d-3p, miR-468-5p, miR-1893-5p, miR-324-3p, miR-324-3p, miR-468-3p, miR-335-3p, miR-681, miR-17-3p, miR-1947 and miR-193a-3p were increased, while others such as miR-1893-3p, miR-1187, miR-31a-3p, miR-191a-3p, miR-1231-5p, miR-210-3p, miR-335-5p, miR-31a-5p and miR-6004 were decreased by more than 2-fold in MI tissues compared to normal cardiomyocytes (**Figure 1C**). It is interesting that miR-328-3p significantly increased in both MI cardiomyocytes and adjacent cardiomyocytes compared to normal cardiomyocytes. Considering that the MI cardiomyocytes and normal cardiomyocytes cannot direct contact entirely, we hypothesized the reason for this phenomenon is exosomes transfer miR-328-3p from MI cardiomyocytes to normal cardiomyocytes. To explore the reason, we collected and isolated exosomes from the MI tissues and normal cardiomyocytes. The exosomes were observed by transmission electron microscopy (**Figure 1D**). The exosomes were positive for exosomal proteins CD34, CD81, CD44, CD200 and CD105 (**Figure 1E**). We then examined exosomal miRNA expression profile. Total RNAs were extracted and subjected to miRNA microarray. Some exosomal miRNAs including miR-124a-5p, miR-564-3p, miR-438-3p, miR-328-3p, miR-153a-3p, miR-4100 and miR-320-3p were increased, while others such as miR-5404, miR-3455-3p, miR-1226 were decreased by more than 2-fold in MI cardiomyocytes compared to normal cardiomyocytes (**Figure 1F**). MiR-328-3p is the intersection of these three miRNA microarray sets (**Figure 1G**). We selected miR-328-3p, which showed similar expression pattern in vitro and in vivo for further investigation.

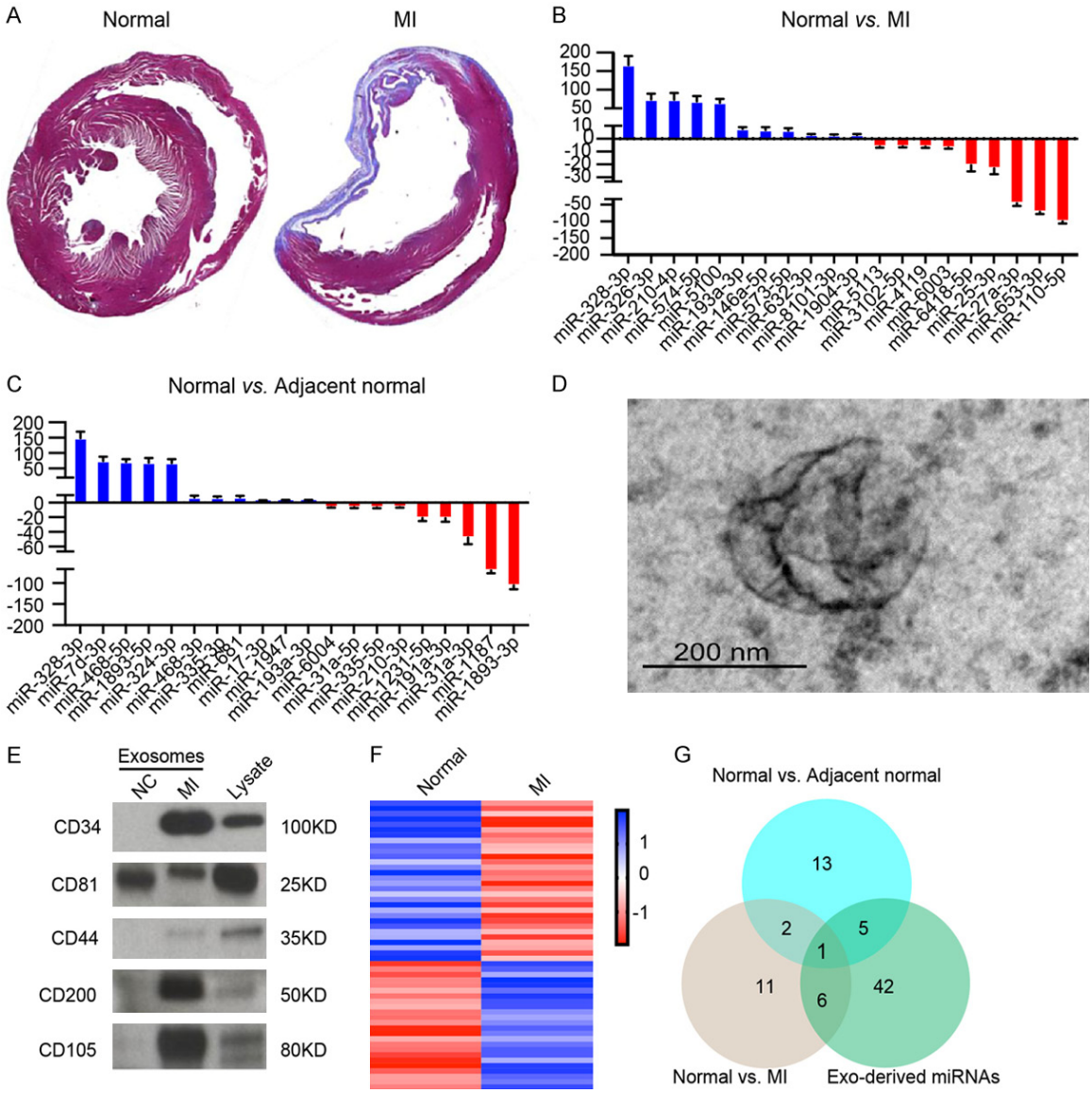

Figure 1. Exosomal miRNAs secreted from cardiomyocytes during MI. (A) Representative images of Masson's trichrome staining of whole heart tissue at 4 weeks after LAD coronary artery ligation surgery. (B) Representative upregulated or downregulated microRNAs from normal heart tissues in contrast to MI heart tissues. (C) Representative upregulated or downregulated microRNAs from normal heart tissues in contrast to MI adjacent normal tissues. (D) Transmission electron microscopy of exosomes derived from heart tissues. Scale bar represents 200 nm. (E) Western blotting analysis of CD34, CD81, CD44, CD200 and CD105 in exosomes from normal heart tissues and MI tissues and lysate of MI cells. Each lane was loaded with 10 μg exosomal protein. (F) RNAseq revealed a different miRNA expression profile of exosomes isolated from MI tissues compared to control exosomes. (G) Intersection of differential miRNA between differential miRNAs of result (B, C and F).

Effect of MI cardiomyocytes-derived exosomes on cardiac apoptosis and morphology

It has long been known that apoptosis is the main feature of MI. Cardiomyocytes apoptosis contributes to MI progression. To explore whether MI cardiomyocytes-derived exosomes promote apoptosis, we analyzed apoptotic level of cardiomyocytes by FACS after treated with increasing concentrations of exosomes form MI cardiomyocytes for 24 hours. The number of apoptotic cells increases after treated with cardiomyocytes-derived exosomes (**Figure 2A**). Cardiomyocytes treaded with exosomes were observed by microscope. Hochest stanning assay showed that the nuclear fragmentation

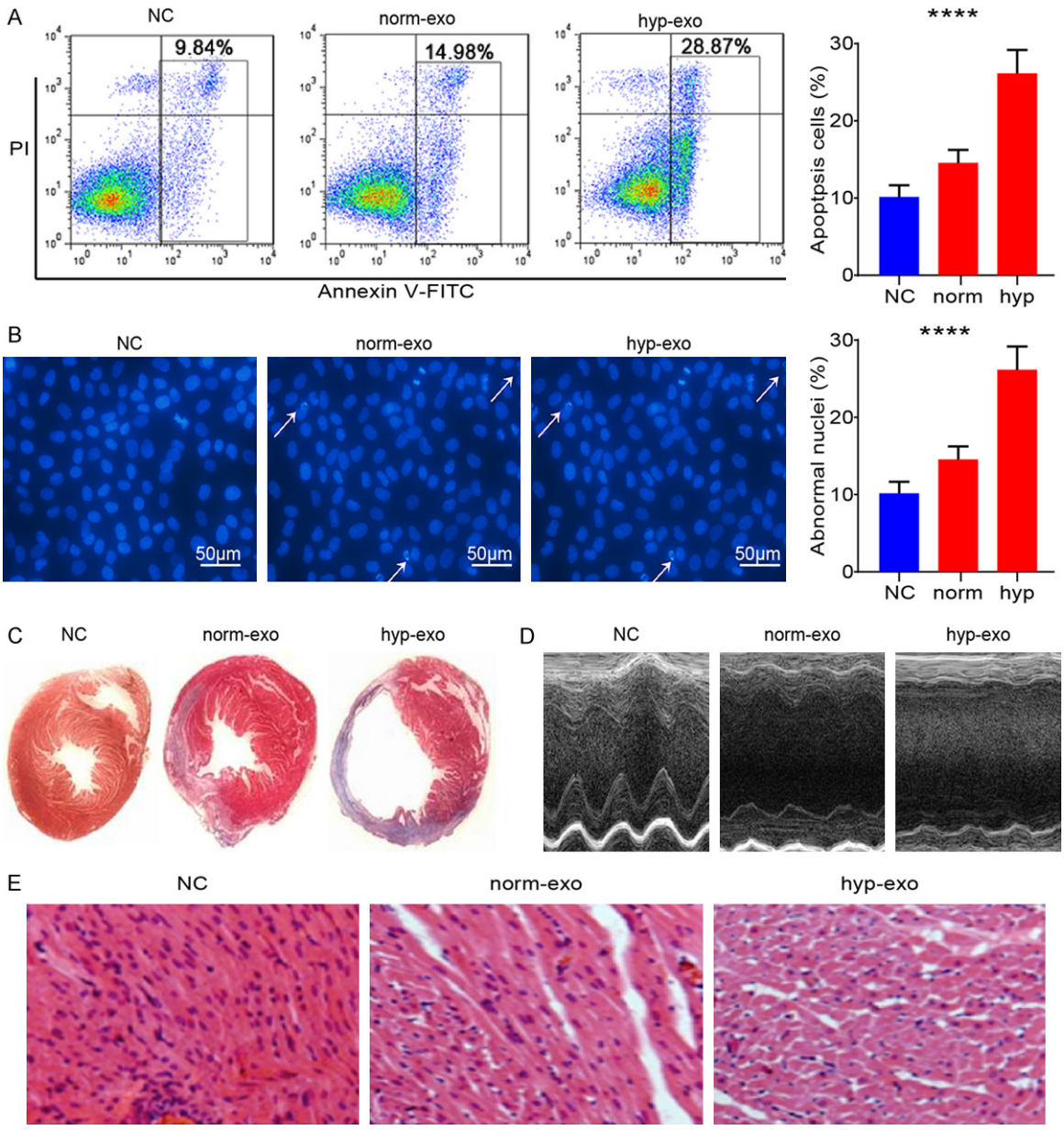

Figure 2. Exosomes from MI cardiomyocytes enhances apoptosis in cardiomyocytes. H9C2 cells were treated with different concentration ($1*10^6$/ml for normal concentration and $1*10^7$/ml for high concentration) of exosomes from MI cardiomyocytes for 24 hours. A. Cells were stained with Annexin V-FITC/PI, and apoptosis was analyzed by flow cytometry (****P < 0.001.). B. The Hochest stanning assay was performed. Images were captured by fluorescence microscopy. The blue color marks the nucleus of all cells. The percentage of nuclear fragmentation cells is reported (****P < 0.001.). C. Representative Masson's trichrome-stained histological sections to measure infarct size 10 days after coronary ligation. D. Echocardiographic measurements were performed 10 days after coronary ligation. Representative M-mode images at the papillary muscle level were recorded for various groups. E. Representative H&E-stained histological sections (magnification of ×200) of left ventricle from rats subjected to treatment for 10 consecutive days with MI cardiomyocytes-derived exosomes. Mean ± SEM.

were increased in cells undergoing apoptosis after treated with MI cardiomyocytes-derived exosomes, respectively (**Figure 2B**). This finding shows that MI cardiomyocytes-derived exosomes treatment enhances apoptosis in cardiomyocytes. Based on the Masson's trichrome staining (**Figure 2C**), the exosomes treated group had a remarkably reduced infarct size in the left ventricle compared with the control group at 10 days following exosomes transplan-

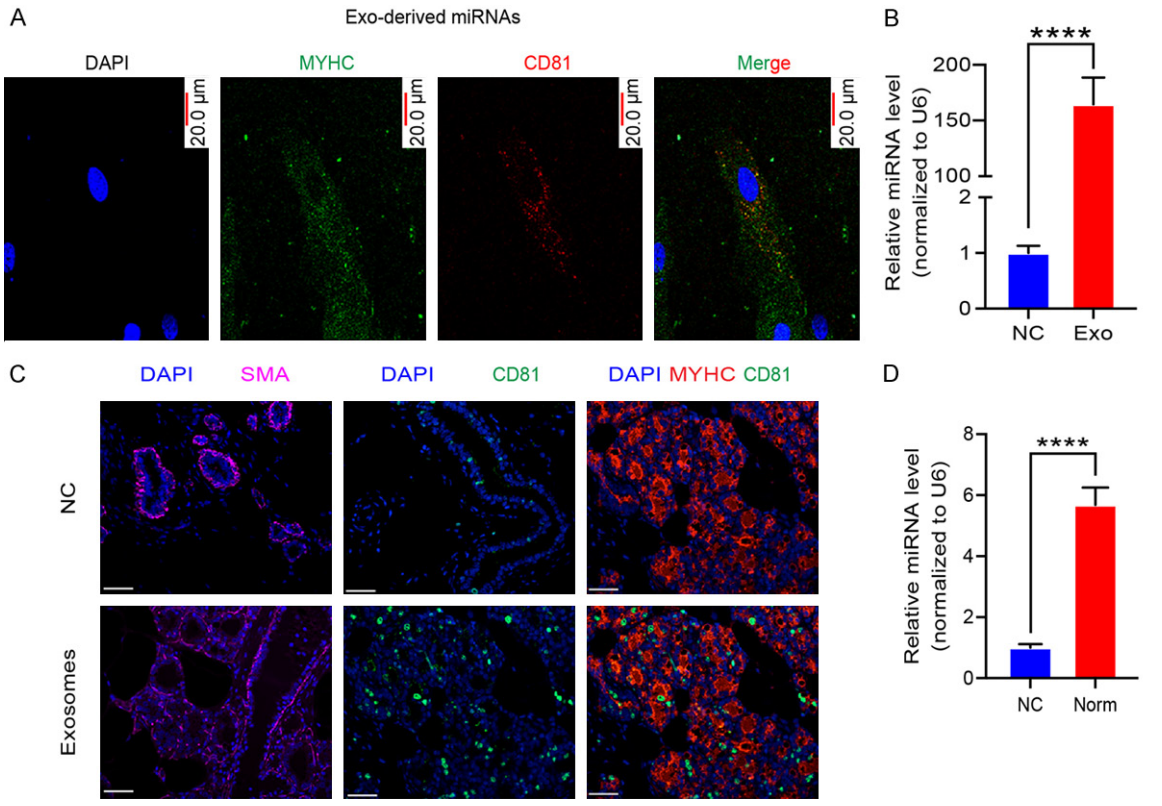

Figure 3. The exosomal miR-328-3p was transferred from MI cardiomyocytes to the normal cardiomyocytes. A. Fluorescently labeled exosomes entered into cardiomyocytes. Representative images were filmed after cells were fixed and stained (magnification, 400×). B. The expression of miR-328-3p, in cardiomyocytes after treatment measured by Quantitative real-time PCR. Normal cardiomyocytes were treated with MI cardiomyocytes-secreted exosomes. Experiments were performed in triplicate. (****P < 0.001.). C. Fluorescently labeled exosomes entered into cardiomyocytes. Representative images were filmed after cells were fixed and stained (magnification, 400×). D. The expression of exosomal miR-328-3p measured by Quantitative real-time PCR (****P < 0.001.). Experiments were performed in triplicate. Mean ± SEM.

tation. Cardiac function was evaluated at 10 days following exosomes delivery according to echocardiography assays. The LVIDd and LVIDs in the exosomes treated group were significantly lower than that in the control group (**Figure 2D**). To confirm these results, H&E-stained histological sections of left ventricle from rats were captured after 10 days following exosomes delivery. Morphometric analysis revealed that treatment with exosomes increased the space between muscle fibers (**Figure 2E**). These results showed that MI cardiomyocytes-derived exosomes aggravate apoptosis of cardiomyocytes and accelerate MI.

Cardiomyocytes uptake MI cardiomyocytes-derived exosomes

To examine whether exosomes secreted by MI cardiomyocytes translocated into normal cardiomyocytes. The MI cardiomyocytes-derived exosomes were labeled with CD81 and were incubated with normal cardiomyocytes. The fluorescent exosomes entered the cardiomyocytes (**Figure 3A**). MiR-328-3p, carried by exosomes, was increased in the normal cardiomyocytes after treated with MI cardiomyocytes-derived exosomes (**Figure 3B**). The treatment with MI cardiomyocytes medium also resulted in the fluorescent exosomes entered the cardiomyocytes (**Figure 3C**) and upregulated expression of miR-328a-3p (**Figure 3D**). These results showed that normal cardiomyocytes can uptake exosomes derived from MI cardiomyocytes.

Effect of exosomal miR-328-3p on cardiac apoptosis and morphology

To explore whether exosomal miR-328-3p promotes apoptosis, we analyzed apoptotic level of cardiomyocytes by FACS after treated with

exosomes form MI cardiomyocytes and/or miR-328-3p inhibitor for 24 hours. The number of apoptotic cells increases after treated with exosomes form MI cardiomyocytes and miR-328-3p inhibitor reversed this phenomenon (**Figure 4A**). Cardiomyocytes apoptosis were observed by microscope. Hochest stanning assay showed that the nuclear fragmentation were increased in cardiomyocytes after treated with MI cardiomyocytes-derived exosomes and miR-328-3p inhibitor suppresses apoptosis promoting effect of MI cardiomyocytes-derived exosomes (**Figure 4B**). This finding shows that miR-328-3p inhibitor inhibited apoptosis promoting effect of MI cardiomyocytes-derived exosomes. Based on the Masson's trichrome staining (**Figure 4C**), the exosomes treated group had a remarkably reduced infarct size in the left ventricle compared with the control group at 10 days following exosomes transplantation and miR-328-3p inhibitor treatment delayed MI progression (**Figure 4C**). 10 days following exosomes and/or miR-328-3p inhibitor treatment, cardiac function was evaluated according to echocardiography assays. The LVIDd and LVIDs in the exosomes treated group were significantly lower than that in the control group and miR-328-3p inhibitor treatment retained cardiac function (**Figure 4D**). To confirm these results, we captured H&E-stained histological sections of left ventricle after 10 days following exosomes and/or miR-328-3p inhibitor treatment. Morphometric analysis revealed that treatment with exosomes increased the space between muscle fibers and miR-328-3p inhibitor reversed this phenomenon (**Figure 4E**). These results showed that miR-328-3p inhibitor reversed the apoptosis promoting and MI acceleration effect of MI cardiomyocytes-derived exosomes. It indicated that miR-328-3p is main MI promoting effector of MI cardiomyocytes-derived exosomes.

MiR-328-3p promotes MI by caspase signaling

To uncover the mechanism driving the miR-328-3p pro-apoptosis effect on cardiomyocytes, we analyzed transcriptomic profiles in H9C2 cells treated with MI cardiomyocytes-derived exosomes (**Figure 5A**). We transferred GFP labeled miR-328-3p overexpression lentivirus into cardiomyocytes. The green fluorescent positive cardiomyocytes were collected by flow cytometry cell sorting and subjected to RNA sequencing analysis (**Figure 5B**). Gene expression profiling was performed on cardiomyocytes collected from 3 samples for each group. Compared to cardiomyocytes treated with medium without exosomes, cardiomyocytes treated with MI cardiomyocytes-derived exosomes had 59 upregulated and 126 downregulated genes (**Figure 5A**, left). The upregulated genes were enriched in the Caspase pathway (**Figure 5A**, right). We further found that the miR-328-3p overexpressed cardiomyocytes had 61 upregulated and 49 downregulated genes compared to control group (**Figure 5B**, left). These upregulated genes were also enriched in the Caspase pathway (**Figure 5B**, right). Z-DEVD-FMK is a specific and irreversible Caspase-3 inhibitor. We treated cardiomyocytes with miR-328-3p overexpression lentivirus and/or Z-DEVD-FMK. We then examined whether miR-328-3p regulate the Caspase pathway. Western blot assays showed that miR-328-3p overexpression lentivirus active Caspase pathway by increasing cleaved-Caspase 3 and Z-DEVD-FMK treatment effectively reversed it (**Figure 5C**). The apoptotic level of cardiomyocytes by FACS increased with miR-328-3p overexpression lentivirus treatment and Z-DEVD-FMK reversed this phenomenon (**Figure 5D**, **5E**). To confirm these results, we captured H&E-stained histological sections of left ventricle after 10 days following miR-328-3p overexpression lentivirus and/or Z-DEVD-FMK treatment. Morphometric analysis revealed that treatment with miR-328-3p overexpression lentivirus increased the space between muscle fibers and Z-DEVD-FMK reversed this phenomenon (**Figure 5F**). These results showed that the Z-DEVD-FMK could reverse the apoptosis progression induced by miR-328-3p, indicating that the activation of Caspase pathway by miR-328-3p was important mechanism of cardiomyocytes and MI.

Discussion

Exosomes are the major mediators of cell-cell communication because they can be captured by neighboring cells [18]. The direct transfer of exosomal miR-193a-3p, miR210-3p and miR-5100 from MI cardiomyocytes to neighboring cardiomyocytes enhances apoptosis. Emerging evidence has demonstrated the feasibility of circulating miRNAs as robust, non-invasive biomarkers for the diagnosis of diseases, such as cancer [19]. Due to their presence in the bodily fluids, exosomes are considered candidate bio-

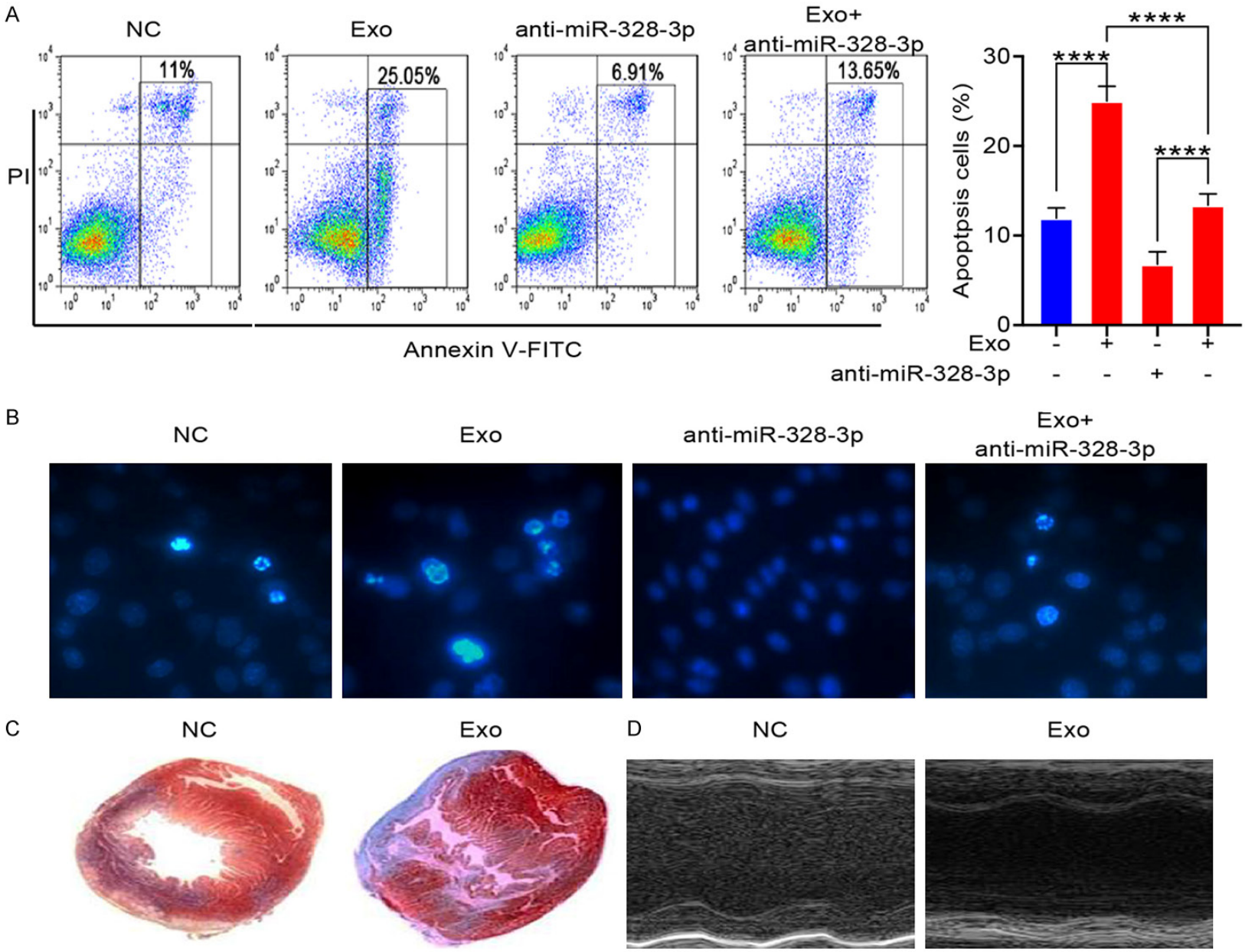
A
NC
Exo
anti-miR-328-3p
Exo+
anti-miR-328-3p
11%
25.05%
6.91%
13.65%
PI
Annexin V-FITC
Apoptpsis cells (%)
30
20
10
0
****
****
****
Exo
anti-miR-328-3p
B
NC
Exo
anti-miR-328-3p
Exo+
anti-miR-328-3p
C
NC
Exo
D
NC
Exo

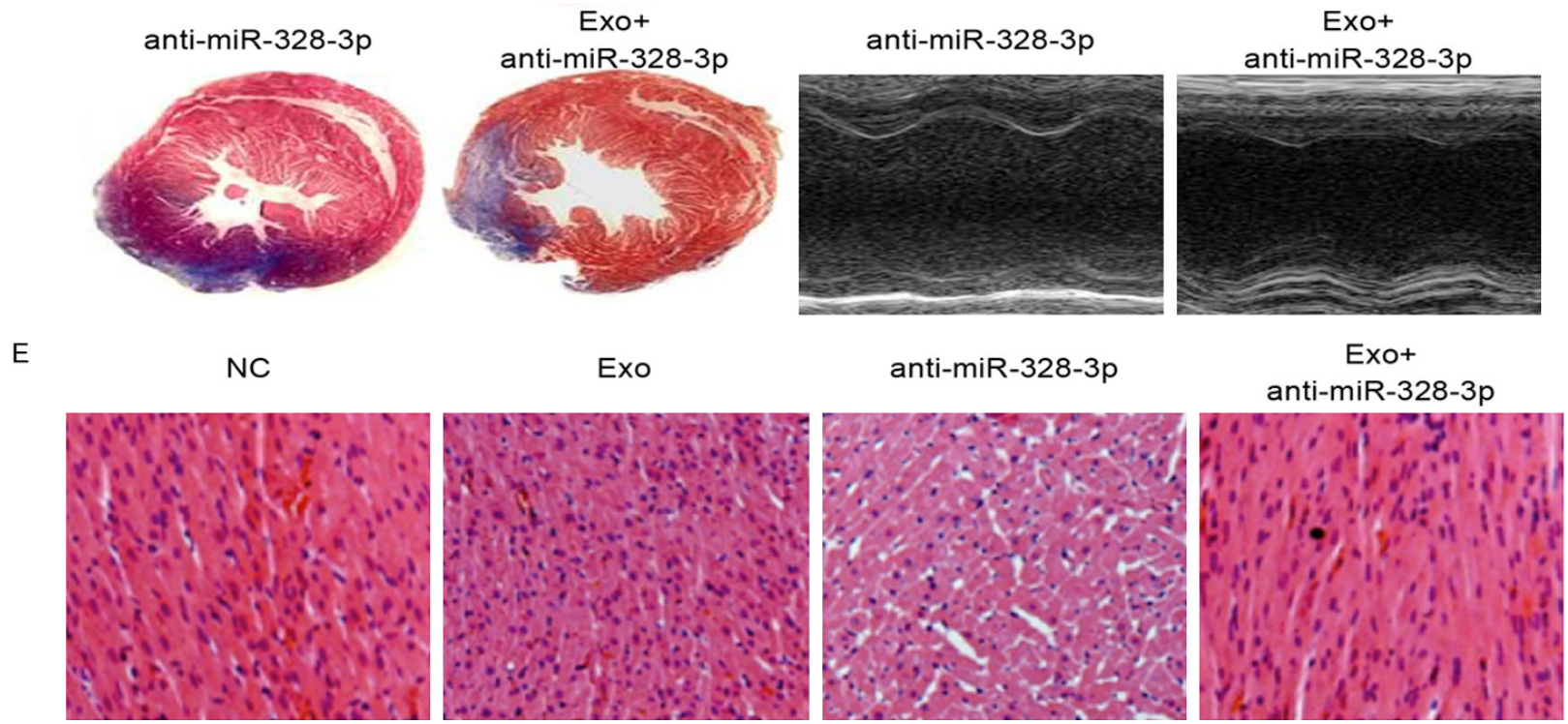

Figure 4. MiR-328-3p enhances apoptosis in cardiomyocytes and MI promoting effect. H9C2 cells were treated with MI cardiomyocytes-derived exosomes and/or miR-328-3p inhibitor for 24 hours. A. Cells were stained with Annexin V-FITC/PI, and apoptosis was analyzed by flow cytometry (****P < 0.001.). B. The Hochest stanning assay was performed. Images were captured by fluorescence microscopy. The blue color marks the nucleus of all cells. The percentage of nuclear fragmentation cells is reported. C. Representative Masson's trichrome-stained histological sections to measure infarct size 10 days after coronary ligation. D. Echocardiographic measurements were performed 10 days after coronary ligation. Representative M-mode images at the papillary muscle level were recorded for various groups. E. Representative H&E-stained histological sections (magnification of ×200) of left ventricle from rats subjected to treatment for 10 consecutive days with MI cardiomyocytes-derived exosomes. Mean ± SEM.

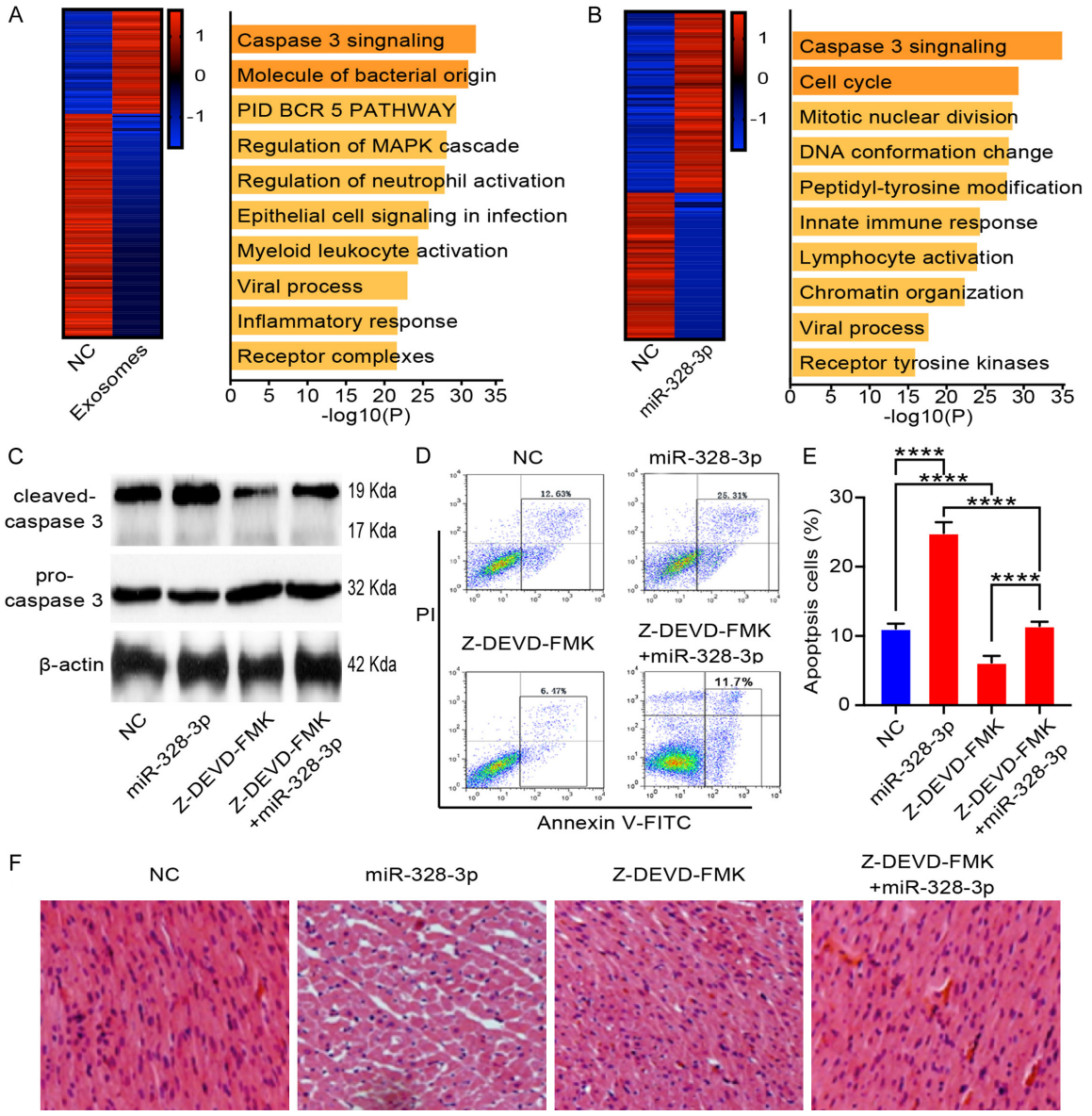

Figure 5. miR-328-3p promotes apoptosis through Caspase signaling pathway. A. H9C2 cells were treated with MI cardiomyocytes-derived exosomes. Gene expression profiling was performed (left) and gene enrichment were analyzed (right). B. Gene expression profiling of miR-328-3p overexpressed cardiomyocytes (left) and upregulated genes enrichment (right). C. Protein expression of cleaved-Caspase 3 and pro-Caspase 3 were measured by Western blot analysis. Cells were treated with miR-328-3p overexpression lentivirus and/or Z-DEVD-FMK. β-actin was used as the internal control. D. Cell apoptosis was measured by flow cytometry. The increased apoptosis induced by miR-328-3p overexpression lentivirus was reversed by Z-DEVD-FMK. E. Apoptosis proportion of cardiomyocytes was counted. Cells were treated with miR-328-3p overexpression lentivirus and/or Z-DEVD-FMK. Experiments were performed in triplicate. ****P < 0.001. F. Space between muscle fibers measured by morphometric analysis. The Z-DEVD-FMK could reverse the enhanced space between muscle fibers induced by miR-328-3p overexpression lentivirus.

markers [20]. The use of exosomal miRNAs as biomarkers, instead of one unique miRNA, has been considered to be a more powerful tool [21]. In this study, we found that MI cardiomyocytes secreted exosomes, which can be taken into normal cardiomyocytes and accelerated apoptosis. Further analyze showed that miR-328-3p significantly increase in MI cardiomyocytes derived exosomes, which indicated that miR-328-3p is the important regulator of cardiomyocytes apoptosis.

miR-328-3p has been reported to be involved in proliferation, apoptosis, and motility [22].

The current study provides evidences that miR-328-3p in osteosarcoma cells can inhibited proliferation and promoted apoptosis by down-regulating H2AX [23]. And overexpression of miR-328-3p inhibited the cell growth and proliferation of bladder cancer cells [24]. Additional analysis showed that miR-328-3p could decrease the migration and tumor formation, but promote the apoptosis of hepatocellular carcinoma cells [25]. More importantly, knock-down of miR-328-3p exhibited the opposite effects compared with overexpression of miR-328-3p. In the presents study, we first studied miR-328-3p expression in the MI, and found miR-328-3p might be a vital target in treating MI. Functional study demonstrated that overexpression of miR-328-3p promoted the development of MI.

miRNA can be transferred between MI cardiomyocytes and normal cardiomyocytes, which results in efficient silencing of mRNAs to reprogram the target cell transcriptome [26]. For instance, exosomal miR-1247-3p derived from hepatocellular carcinoma cells can be delivered to cancer-associated fibroblast and prime cancer-associated fibroblast activation, consequently promotes hepatocellular carcinoma metastasis [27]. Exosome-mediated miR-19a transferred from astrocytes to tumor cells hampered PTEN expression and aggressive outgrowth in the brain. In summary, these studies suggest that exosomes-mediated transfer of miRNA between cancer cells and stromal cells is essential for cancer progression [28]. Our results of Gene chip showed that miR-328-3p levels in MI cardiomyocytes and adjacent normal cardiomyocytes were positively correlated, based on which we raised the hypothesis that miR-328-3p can be transferred from MI cardiomyocyte to adjacent normal cardiomyocytes via exosomes. In addition, we observed fluorescence in normal cardiomyocytes incubated with exosomes from MI cardiomyocytes that were transfected with CD81-labeled exosomes. These results showed that MI cardiomyocytes-secreted exosomal miR-328-3p can be transferred to cardiomyocytes.

In this study, we found miR-328-3p promotes the activation of the Caspase pathway. Caspases are found inside the cell as inactive preforms, upon which cleavage of an active Caspase becomes the enzymatically-active protein [29]. Caspase-3, a hallmark of apoptosis, has been detected in inflammatory diseases, including rheumatoid arthritis [30]. In the periodontium, the expression of apoptosis-associated genes has been shown to increase when healthy gingival tissue is exposed to pathogenic periodontal bacteria [31]. Therefore, the present study was performed to estimate and correlate the GCF and serum levels of Caspase-3 to assess the apoptotic activity in periodontal health and disease, and to explore Caspase-3 as a biomarker of periodontal disease and its progression [32]. Our study accumulated genes regulated by miR-328-3p and evaluate the role of Caspase-3 in MI. The difference in levels of Caspase-3 was regulated by miR-328-3p. The results of our study showed that activation of Caspase-3 by miR-328-3p plays a critical role in cardiomyocytes apoptosis. Z-DEVD-FMK, Caspase-3 inhibitor, could reverse the apoptosis progression induced by miR-328-3p, indicating that the activation of Caspase pathway by miR-328-3p was important mechanism of cardiomyocytes and MI. Thus, considering the effect of Z-DEVD-FMK as MI treatment, a systemic clinical trial is urgently needed.

Conclusions

In summary, cardiomyocytes-derived exosomal miR-328-3p was upregulated during MI. Exosome-mediated transfer of miR-328-3p could promote apoptosis of cardiomyocytes by activating Caspase-3 signaling. These exosomal miR-328-3p may be promising noninvasive biomarker and potential therapeutic target for MI.

Disclosure of conflict of interest

None.

Abbreviations

MI, myocardial infarction; miRNAs, microRNAs; LAD, left anterior descending; TUNEL, TdT-UTP nick end labeling; TEM, Transmission electron microscopy; LVEDD, left ventricular end-diastolic dimension; LVESD, left ventricular end-systolic diameter; 2D, two-dimensional; LV, left ventricle; FITC, Fluorescin isothiocyanate; PI, propidium iodide.

Address correspondence to: Jiechun Huang, Department of Cardiothoracic Surgery, Huashan Hospital of Fudan University, 12th Wulumuqi Road, Shanghai 200040, PR China. E-mail: cnsdream@163.com

References

[1] Prasad M, Corban MT, Henry TD, Dietz AB, Lerman LO and Lerman A. Promise of autologous CD34+ Stem/progenitor cell therapy for treatment of cardiovascular disease. Cardiovasc Res 2020; 116: 1424-1433.

[2] Xu S, Kamato D, Little PJ, Nakagawa S, Pelisek J and Jin ZG. Targeting epigenetics and non-coding RNAs in atherosclerosis: from mechanisms to therapeutics. Pharmacol Ther 2019; 196: 15-43.

[3] Huang C, Tu W, Fu Y, Wang J and Xie X. Chemical-induced cardiac reprogramming in vivo. Cell Res 2018; 28: 686-689.

[4] Mihalko E, Huang K, Sproul E, Cheng K and Brown AC. Targeted treatment of ischemic and fibrotic complications of myocardial infarction using a dual-delivery microgel therapeutic. ACS Nano 2018; 12: 7826-7837.

[5] Mi L, Sun Y, Shi L and Li T. Hemin-bridged MOF interface with double amplification of G-Quadruplex payload and DNAzyme catalysis: ultrasensitive lasting chemiluminescence microRNA imaging. ACS Appl Mater Interfaces 2020; 12: 7879-7887.

[6] Wernly B, Paar V, Aigner A, Pilz PM, Podesser BK, Forster M, Jung C, Hofbauer JP, Tockner B, Wimmer M, Kraus T, Motloch LJ, Hackl M, Hoppe UC, Kiss A and Lichtenauer M. Anti-CD3 antibody treatment reduces scar formation in a rat model of myocardial infarction. Cells 2020; 9: 295.

[7] Breglio AM, May LA, Barzik M, Welsh NC, Francis SP, Costain TQ, Wang L, Anderson DE, Petralia RS, Wang YX, Friedman TB, Wood MJ and Cunningham LL. Exosomes mediate sensory hair cell protection in the inner ear. J Clin Invest 2020; 130: 2657-2672.

[8] Gao L, Mei S, Zhang S, Qin Q, Li H, Liao Y, Fan H, Liu Z and Zhu H. Cardio-renal exosomes in myocardial infarction serum regulate proangiogenic paracrine signaling in adipose mesenchymal stem cells. Theranostics 2020; 10: 1060-1073.

[9] Kanada M, Bachmann MH, Hardy JW, Frimannson DO, Bronsart L, Wang A, Sylvester MD, Schmidt TL, Kaspar RL, Butte MJ, Matin AC and Contag CH. Differential fates of biomolecules delivered to target cells via extracellular vesicles. Proc Natl Acad Sci U S A 2015; 112: E1433-1442.

[10] Kuwabara Y, Ono K, Horie T, Nishi H, Nagao K, Kinoshita M, Watanabe S, Baba O, Kojima Y, Shizuta S, Imai M, Tamura T, Kita T and Kimura T. Increased microRNA-1 and microRNA-133a levels in serum of patients with cardiovascular disease indicate myocardial damage. Circ Cardiovasc Genet 2011; 4: 446-454.

[11] Aurora AB, Mahmoud AI, Luo X, Johnson BA, van Rooij E, Matsuzaki S, Humphries KM, Hill JA, Bassel-Duby R, Sadek HA and Olson EN. MicroRNA-214 protects the mouse heart from ischemic injury by controlling Ca(2)(+) overload and cell death. J Clin Invest 2012; 122: 1222-1232.

[12] van Balkom BW, de Jong OG, Smits M, Brummelman J, den Ouden K, de Bree PM, van Eijndhoven MA, Pegtel DM, Stoorvogel W, Wurdinger T and Verhaar MC. Endothelial cells require miR-214 to secrete exosomes that suppress senescence and induce angiogenesis in human and mouse endothelial cells. Blood 2013; 121: 3997-4006, S3991-3915.

[13] Narjala A, Nair A, Tirumalai V, Hari Sundar GV and Shivaprasad PV. A conserved sequence signature is essential for robust plant miRNA biogenesis. Nucleic Acids Res 2020; 48: 3103-3118.

[14] Ahmed F, Ijaz B, Ahmad Z, Farooq N, Sarwar MB and Husnain T. Modification of miRNA Expression through plant extracts and compounds against breast cancer: mechanism and translational significance. Phytomedicine 2020; 68: 153168.

[15] Liu Y, Yang L, Yin J, Su D, Pan Z, Li P and Wang X. MicroRNA-15b deteriorates hypoxia/reoxygenation-induced cardiomyocyte apoptosis by downregulating Bcl-2 and MAPK3. J Investig Med 2018; 66: 39-45.

[16] Shiraishi H, Okamoto H, Yoshimura A and Yoshida H. ER stress-induced apoptosis and caspase-12 activation occurs downstream of mitochondrial apoptosis involving Apaf-1. J Cell Sci 2006; 119: 3958-3966.

[17] Kilkenny C, Browne WJ, Cuthill IC, Emerson M and Altman DG. Improving bioscience research reporting: the ARRIVE guidelines for reporting animal research. Osteoarthritis Cartilage 2012; 20: 256-260.

[18] Kalluri R and LeBleu VS. The biology, function, and biomedical applications of exosomes. Science 2020; 367: eaau6977.

[19] Dai W, Su L, Lu H, Dong H and Zhang X. Exosomes-mediated synthetic Dicer substrates delivery for intracellular Dicer imaging detection. Biosens Bioelectron 2020; 151: 111907.

[20] Peng XX, Yu RY, Wu X, Wu SY, Pi C, Chen ZH, Zhang XC, Gao CY, Shao YW, Liu L, Wu YL and Zhou Q. Correlation of plasma exosomal microRNAs with the efficacy of immunotherapy in EGFR/ALK wild-type advanced non-small cell lung cancer. J Immunother Cancer 2020; 8: e000376.

[21] Wu HJ, Hao M, Yeo SK and Guan JL. FAK signaling in cancer-associated fibroblasts promotes breast cancer cell migration and metastasis by exosomal miRNAs-mediated intercellular communication. Oncogene 2020; 39: 2539-2549.

[22] Wu G, Wang Y, Yang Y, Shi Y, Sun J, Xu Y, Luo T and Le G. Dietary methionine restriction upregulates endogenous H2 S via miR-328-3p: a potential mechanism to improve liver protein metabolism efficiency in a mouse model of high-fat-diet-induced obesity. Mol Nutr Food Res 2019; 63: e1800735.
[23] Yang Z, Wa QD, Lu C, Pan W, Lu Z and Ao J. miR3283p enhances the radiosensitivity of osteosarcoma and regulates apoptosis and cell viability via H2AX. Oncol Rep 2018; 39: 545-553.
[24] Yan T and Ye XX. MicroRNA-328-3p inhibits the tumorigenesis of bladder cancer through targeting ITGA5 and inactivating PI3K/AKT pathway. Eur Rev Med Pharmacol Sci 2019; 23: 5139-5148.
[25] Li JZ, Li J and Liu BZ. MicroRNA-328-3p inhibits malignant progression of hepatocellular carcinoma by regulating MMP-9 level. Eur Rev Med Pharmacol Sci 2019; 23: 9331-9340.
[26] Foinquinos A, Batkai S, Genschel C, Viereck J, Rump S, Gyongyosi M, Traxler D, Riesenhuber M, Spannbauer A, Lukovic D, Weber N, Zlabinger K, Hasimbegovic E, Winkler J, Fiedler J, Dangwal S, Fischer M, de la Roche J, Wojciechowski D, Kraft T, Garamvolgyi R, Neitzel S, Chatterjee S, Yin X, Bar C, Mayr M, Xiao K and Thum T. Preclinical development of a miR-132 inhibitor for heart failure treatment. Nat Commun 2020; 11: 633.
[27] Fang T, Lv H, Lv G, Li T, Wang C, Han Q, Yu L, Su B, Guo L, Huang S, Cao D, Tang L, Tang S, Wu M, Yang W and Wang H. Tumor-derived exosomal miR-1247-3p induces cancer-associated fibroblast activation to foster lung metastasis of liver cancer. Nat Commun 2018; 9: 191.
[28] Zhang L, Zhang S, Yao J, Lowery FJ, Zhang Q, Huang WC, Li P, Li M, Wang X, Zhang C, Wang H, Ellis K, Cheerathodi M, McCarty JH, Palmieri D, Saunus J, Lakhani S, Huang S, Sahin AA, Aldape KD, Steeg PS and Yu D. Microenvironment-induced PTEN loss by exosomal microRNA primes brain metastasis outgrowth. Nature 2015; 527: 100-104.
[29] Gunther SD, Fritsch M, Seeger JM, Schiffmann LM, Snipas SJ, Coutelle M, Kufer TA, Higgins PG, Hornung V, Bernardini ML, Honing S, Kronke M, Salvesen GS and Kashkar H. Cytosolic Gram-negative bacteria prevent apoptosis by inhibition of effector caspases through lipopolysaccharide. Nat Microbiol 2020; 5: 354-367.
[30] Bhagya KP, Aswathy RJ, Radhakrishnan K, Sengottaiyan J and Kumar PG. Autoimmune regulator enhanced the expression of Caspase-3 and did not induce massive germ cell apoptosis in GC1-Spg cells. Cell Physiol Biochem 2020; 54: 40-52.
[31] Buschhaus JM, Humphries B, Luker KE and Luker GD. A caspase-3 reporter for fluorescence lifetime imaging of single-cell apoptosis. Cells 2018; 7: 57.
[32] Adekambi T, Ibegbu CC, Cagle S, Ray SM and Rengarajan J. High frequencies of caspase-3 expressing mycobacterium tuberculosis-specific CD4(+) T cells are associated with active tuberculosis. Front Immunol 2018; 9: 1481.